Desalination and Water Treatment
www.deswater.com
doi: 10.5004/dwt.2023.29273

284 (2023) 19–26
February

How membrane fouling evolves during electrodialysis treatment of cold-rolling wastewater?

Yinghua Li*, Shijie Zhang, Jie Qian, Fei Su, Haibo Li

School of Resources and Civil Engineering, Northeastern University, Shenyang 110004, China, Tel.: +86-24-83679128; Fax: +86-24-83679128; emails: liyinghua1028@126.com (Y. Li), 741068503@qq.com (S. Zhang), 2010383@stu.neu.edu.cn (J. Qian), sufei0908@163.com (F. Su), graceli_2003@163.com (H. Li)

Received 8 August 2022; Accepted 9 December 2022

ABSTRACT

Membrane fouling is a serious concern in cold-rolling wastewater treatment using electrodialysis (ED). In this study, a commonly used anion exchange membrane was selected, and the evolution of fouling behavior was evaluated by contact angle, atomic force microscope (AFM), scanning electron microscope-energy-dispersive X-ray spectrometer (SEM-EDS), X-ray photoelectron spectroscopy (XPS) and attenuated total refraction-Fourier transform infrared (ATR-FTIR). Furthermore, mechanism of hybrid pollution by organic and inorganic contaminants was presented. Representative regeneration methods were carried out to investigate the removal of pollutants. The results showed that compared with the uncontaminated ED, the electrical resistance of desalination compartment increased by 5.49% and 10.42% after 48 and 96 h contamination, respectively. Meanwhile, Cl^- recovery rate decreased from 64.33% ± 0.02% (uncontaminated membrane) to 58.58% ± 0.10% (contaminated for 48 h) and 55.32% ± 0.52% (contaminated for 96 h). Results from SEM-EDS, AFM, XPS and FTIR revealed that the interaction between organic (dichloromethane, dichloroacetaldehyde, chloromethylsulfonyl chloride) and inorganic fouling (Fe^{2+}) was the central factor in exacerbating membrane fouling, which resulted in more complicated fouling scenarios. It is recommended to remove chemical oxygen demand from membrane surface with 0.1% NaOH followed by 0.025% Na-SDS every 96 h to restore the permeability.

Keywords: Electrodialysis; Cold-rolling wastewater; Membrane fouling; Evolution; Regeneration

1. Introduction

The iron and steel industry are one of the largest energy-intensive and water-intensive industries [1]. Cold-rolling wastewater is a large amount of acidic solution generated in many industrial sectors, especially in iron and steel industries [2,3]. It is a typical hard-to-degrade wastewater with kinds of pollutants and characterized by high acidity, high concentrations of Fe^{2+}, Cl^- and chemical oxygen demand (COD), which can cause serious ecological impacts if discharged directly into natural water bodies [4]. The effective treatment of cold-rolling wastewater can improve the utilization of important water resources, and more importantly, reduce clean water consumption. Various advanced wastewater treatment processes are gradually promoted, and safe discharge of industrial wastewater, even "zero" discharge, has become an important indicator in various planning reviews [3]. Cold-rolling wastewater is usually treated with coagulation, sedimentation followed by aerobic membrane bioreactor (MBR) [2,4]. However, the effluent from MBR typically presents high inorganic salt contents [1]. Meanwhile, most of the application methods that aim to remove or degrade substances in the wastewater, failed to extract useful resources from the wastewater [5,6].

* Corresponding author.

1944-3994/1944-3986 © 2023 Desalination Publications. All rights reserved.

Electrodialysis (ED) is among the most common membrane-based technologies used for recovering irons from water. ED separates salts from aqueous solution through anion exchange membranes (AEMs) and cation exchange membranes (CEMs) under the action of electric field force. Compared with other membrane processes, its pre-treatment requirements are less strict [7,8]. Most importantly, ED can also recover useful substances from wastewater. Due to the development of advanced membranes, ED has been widely used in saline water desalination, acid recovery, and desalination of industrial wastewater [2,9,10]. Nazila et al. [11] studied the extraction of lithium from LiBr solutions by electrodialysis, and the highest concentration of Li^+ obtained in the cathode chamber was 7,654 ppm. Yan et al. [10] investigated the ED membrane stack for processing high-salt solutions through multi-stage batch ED. Through three-stage batch ED, the salt content of the solution was increased from 3.5% to 20.6%, and compared with other methods, relatively low energy consumption was needed.

Although ED has become a potential technology for the treatment of contaminated salt solutions, membrane fouling remains a key issue preventing its further development and application [12–14]. The types of membrane contamination can often be classified as organic fouling, inorganic fouling, colloidal fouling, and biological fouling [15,16]. Moreover, when there are multiple pollutants in wastewater, such as the coexistence of organic and inorganic pollution, membrane pollution will be more significant than single pollution. In particular, when high molecular weight polymers are present, the problem of membrane fouling becomes more prominent. When the contamination of anion exchange membranes by the anionic surfactant sodium dodecylbenzene sulfonate (SDBS) was examined, it was found that when the SDBS concentration was higher than the critical micelle concentration, a contamination layer formed on the membrane surface, which reduced the electrodialysis performance [17]. Next, the studies found that polyacrylamide forms a gel layer on the surface of the membrane, resulting in a decrease in membrane performance [18,19]. This is mainly due to the fact that AEMs are positively charged and generally considered susceptible to fouling by organic matters with different charges [20].

Up to now, there are few reports on the electrodialysis to treat cold-rolling wastewater without any pre-treatments and exploring the membrane fouling process. The purpose of this study was (1) to compare the resistance, Cl^- recovery rate and current efficiency between original and contaminated ED membrane; (2) to carry out membrane fouling experiments with optimized parameters and investigate the evolution of membrane fouling conditions; (3) to develop an optimal regeneration strategy. This research aims to provide valuable insights for the pollution of ED membranes in the recycling of cold-rolling wastewater and provide targeted regeneration strategies.

2. Experimental set-up

2.1. Wastewater

The cold-rolling wastewater was obtained from Angang Steel Company Limited in Liaoning Province, China. The main indexes were pH 1.8–2.0, COD 900–1,000 mg/L, Fe^{2+} 2,000–2,500 mg/L, Cl^- 5,380–7,090 mg/L and conductivity 5.5–6.0 mS/cm. Three main organic pollutants were found: methylene chloride, dichloroacetaldehyde and chloromethylsulfonyl chloride, respectively.

2.2. Equipment

The units of ED experimental set-up contained four repeating unit, each of which was composed of AEMs and CEMs in series (Fig. 1). The effective electrode areas of AEMs and CEMs were 150 cm^2, respectively. Each unit was divided into a dilute compartment and a concentrate compartment. The spacers (polymer) were rectangular with 12 cm width × 12.5 cm height. Stainless steel plate was used as the cathode and a Ti/SnO_2-Sb/PbO_2 electrode was used as the anode. The homogeneous AEMs selected were made by introducing active groups (polyacrylonitrile, polytetrafluoroethylene and polychlorotrifluoroethylene) into an inert carrier (styrene), and the structure was relatively

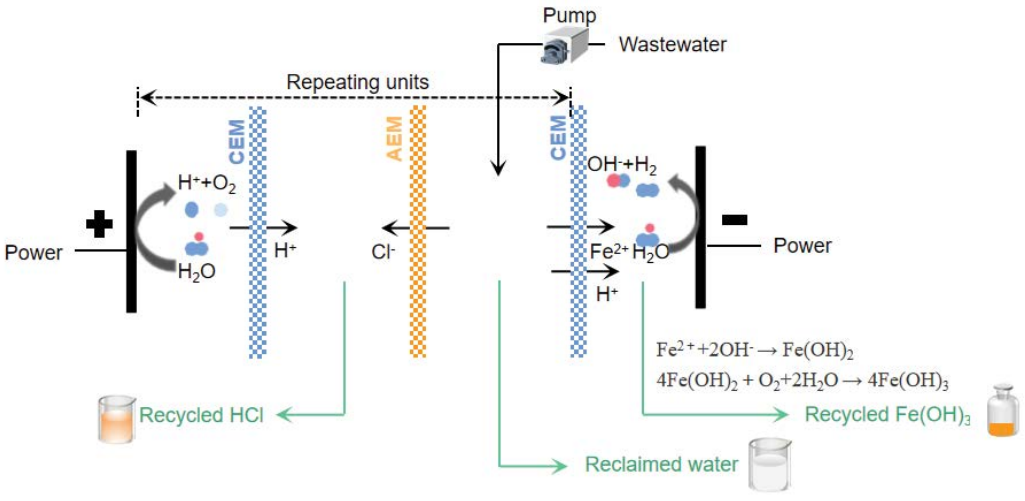

Fig. 1. Schematic diagram of ED configuration.

dense. Before the experiment, the solution in each tank was circulated for 30 min to eliminate the gas bubbles on the membrane surface.

Under the action of electric field, the ions moved through the anion and cation membranes. Fe^{2+} in the desalination chamber reached the cathode chamber and precipitated with OH^- to form $Fe(OH)_2$, which could be easily oxidized to $Fe(OH)_3$ in aerobic environment. H^+ infiltrated through the cation exchange membrane into the concentration chamber on the left side and formed HCl solution with Cl^- thus achieving the purpose of acid recovery. The main reactions are as follows:

At the cathode:

$$2H_2O + 2e^- \rightarrow 2OH^- + H_2 \quad (1)$$

At the anode:

$$2H_2O \rightarrow 4H^+ + O_2 \uparrow + 4e^- \quad (2)$$

In the concentration compartment:

$$Fe^{2+} + 2OH^- \rightarrow Fe(OH)_2 \quad (3)$$

$$4Fe(OH)_2 + O_2 + 2H_2O \rightarrow 4Fe(OH)_3 \quad (4)$$

$$H^+ + Cl^- \rightarrow HCl \quad (5)$$

2.3. Membrane fouling experiments

The parameters used in the membrane fouling experiment were derived from our previous studies (flow rate, 28.8 mL/min; voltage output, 12 V; electrode rinse solution, 0.03 mol/L). Under these conditions, the removal rates of Fe^{2+} and COD can reach 98.5% and 96.1%, respectively. The effluent quality met the "water pollutant discharge standard for iron and steel industry" in China (GB13456-2012) (Fe^{2+} < 100 mg/L and COD < 80 mg/L), which can be directly reused as industrial circulating water without any further treatment.

This study was carried out under the above operating conditions. Two runs were arranged; Runs 1 and 2 for the operation that continuously lasted for 48 and 96 h, respectively. After the contamination experiment, the membranes were dried and stored for subsequent experiments.

2.4. Development of regeneration strategies

Six effective regeneration methods (A–F) were explored in Table 1. Three chemical cleaning reagents: sodium dodecyl sulfonate (Na-SDS), hydrochloric acid (HCl) and sodium hydroxide (NaOH) served as metal chelators, acidic solutions and alkaline solutions, respectively. For the acidic cleaning methods, pH of all samples was controlled to 2; while for the alkaline cleaning methods, pH was set to 12. Analytical grade chemicals were used, and the solutions were prepared using deionized water and finally stored at 4°C.

Six pieces of dried contaminated film were cut for the cleaning strategies explored (1 cm × 1 cm). First, the membranes were placed into 100 mL conical flasks, and then 20 mL cleaning solutions were added as detailed in step 1 and soaked for 2 h. Then the conical flasks were placed simultaneously in a thermostatic shaker incubator at 30°C and run at 80 rpm for 12 h. After that, high-speed rinsing process was simulated for 12 h at 200 rpm. The water samples after rinsing were collected and accurately analyzed.

2.5. Analytical methods

The conductivity, pH, COD, Cl^- and Fe^{2+} concentration were analyzed with reference to the national standard method [4], and the organic pollutants in the wastewater were qualitatively analyzed by GC-MS (QP2010-SE, Japan). The morphology and elemental composition of the film surface were obtained by scanning electron microscopy (Ultra Plus, Germany) equipped with an energy spectrometer (SEM-EDS) and atomic force microscopy (Dimension Icon, USA). As an indicator of the hydrophilicity of the film, the contact angle was measured with an optical contact angle meter (DSA25, Germany). Changes in the functional groups were detected by attenuated total reflection-Fourier transform infrared spectroscopy (ATR-FTIR, Thermo Fisher, USA) with a resolution of 1 cm^{-1} and a range of 350–7,800 cm^{-1}. Conductivity was measured by a conductivity meter, DDS-11A (Shanghai, China). To study the chemical bonding and compositional changes on the AEM surface, the film was measured by X-ray photoelectron spectroscopy (XPS, Thermo K-Alpha, USA). Prior to measurement, all membrane samples were kept dry, and each sample was randomly measured at least three times in two different locations to minimize the effect of surface morphology.

According to the results, Cl^- recovery rate and current efficiency were calculated by Eqs. (6) and (7), respectively.

$$R = \frac{C_1 - C_2}{C_1} \times 100\% \quad (6)$$

Table 1
Regeneration methods tested in this study

Strategy	Method					
	A	B	C	D	E	F
Step 1	Deionized water	0.2% HCl	0.1% NaOH	0.1% NaOH, 0.025% NaSDS	0.1% NaOH	0.1% NaOH, 0.025% NaSDS
Step 2	–	–	–	–	0.2% HCl	0.2% HCl

$$\eta = \frac{FQ\left(C_{in} - C_{out}\right)}{nIt} \times 100\% \quad (7)$$

where R, C_1, and C_2 represents the recovery rate of Cl^- (%), Cl^- concentration in influent (mg/L), and Cl^- concentration in effluent (mg/L), respectively. η represents the current efficiency (%), F = 96,485 C/mol indicates the Faraday constant. Q and I represent the treated volume (L) and current (A), respectively. n = 4 represents the number of repeating unit and t is operation time (s).

3. Results and discussions

3.1. Electrical resistance, salt recovery and current efficiency

In the experiment, the changes of conductivity and recovery rate of Cl^- were monitored sequentially. As shown in Fig. 2, the conductivity of the desalination chamber decreased significantly within 3 h, while the condition of concentrate chamber showed an opposite trend. After 3 h, the conductivity (desalination compartment) of Runs 1 and 2 decreased to 1.92 ± 0.01 and 2.12 ± 0.02 mS/cm, respectively. Compared with the uncontaminated ED, the conductivity increased by 5.49% and 10.42% after 48 and 96 h electrodialysis experiments.

It is generally accepted that the conductivity increased with the total dissolved solids value [1,21]. With the continuous progress of the experiment, substances in the wastewater gradually accumulated on the membrane surface. At the same time, the membrane resistance kept increasing, so the decreased current density resulted in the decrease of desalination performance. Meanwhile, after 3 h of electrodialysis experiments under the same conditions, the Cl^- recovery rate of Run 1 decreased from 64.33% ± 0.02% to 58.58% ± 0.10%, and Run 2 showed a significant decrease to 55.32% ± 0.52%, which further confirmed the occurrence of pollution resulting from long operation (Fig. 3a).

There were two inflection points 1 and 2 on the V-I curve (Fig. 3b). The physical meaning of point 1 was that at this time, the current in the desalination chamber began to be smaller than that in the membrane, and then a current

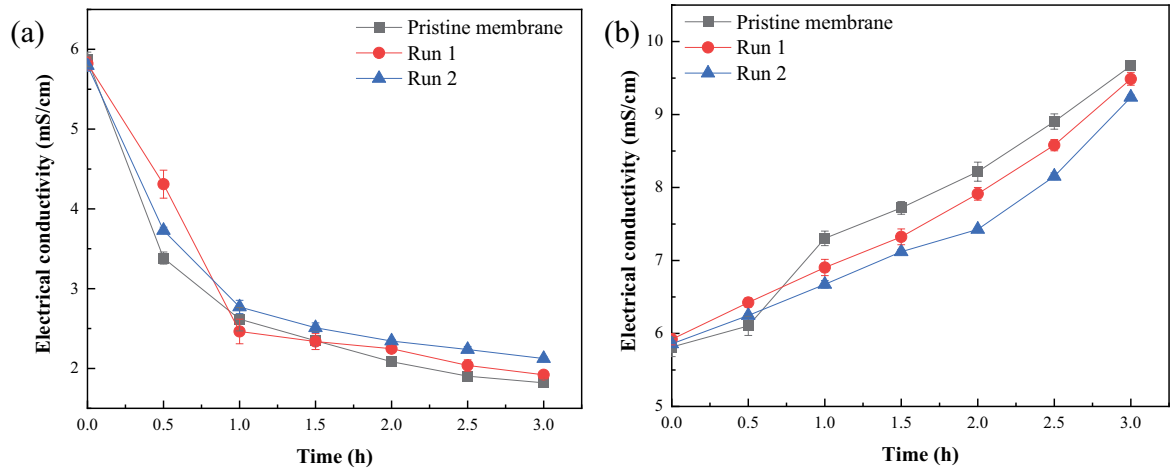

Fig. 2. Electrical resistance with time in (a) desalination chamber and (b) enrichment chamber.

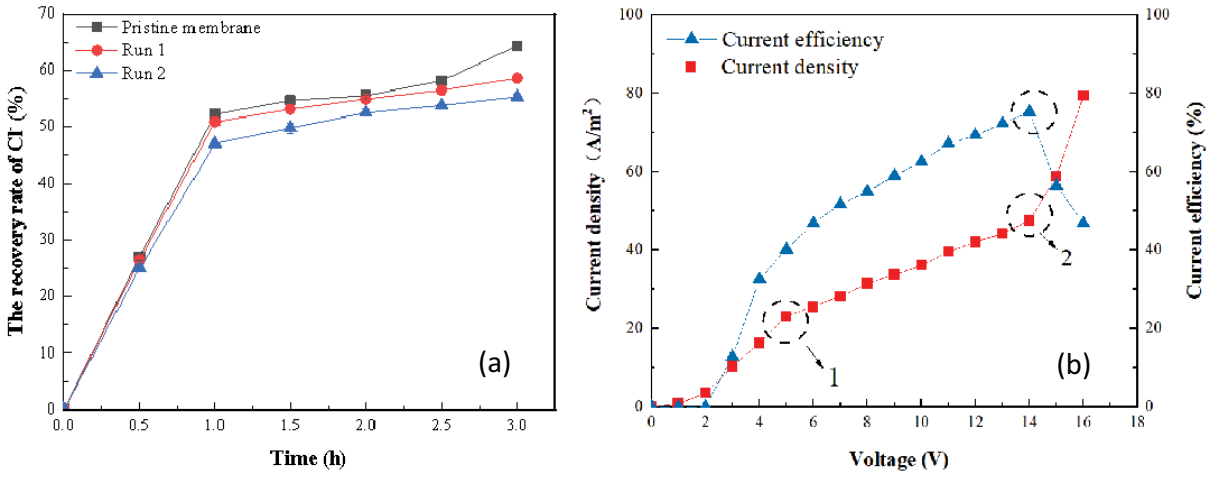

Fig. 3. (a) Recovery rate of Cl^- with time and (b) current efficiency with voltage.

difference and additional potential (also known as concentration difference) formed on both sides of the interface layer [1,11]. Point 2 represented the concentration polarization point. At this time, significant water dissociation occurred in the interface layer. In order to make up for the shortage of ions in the desalination chamber, the additional potential reached a maximum [9], and the corresponding value was the limiting current (14 V in this study).

According to these results, the limiting current density and the corresponding limiting voltage were 47.56 A/m^2 and 14 V, respectively. In practical operation, the value of the operating current density was generally 70%–90% of the limiting current density. Therefore, the operating current density was selected to be 42.14 A/m^2 and the operating voltage was 12 V. The current efficiency reached 75% for the original membrane.

3.2. Fouling evolution

3.2.1. Contact angle analysis

Based on the contact angle (θ) test, significant increases were observed, indicating membrane fouling occurred at the end of the experiment. The contact angle mainly indicated the changes in hydrophilicity and hydrophobicity of the membrane caused by the adhesion of pollutants to the membrane [16,19,22]. When water drops fall from the instrument, the first direct contact is with the contamination layer on the surface of the membrane, not the surface of the membrane itself. Contact angle increased from 90.8° (Original) to 105° (Run 1) and 109° (Run 2), indicating that hydrophobic pollutants in the wastewater were an important source of organics. The conclusion was consistent with previous reports [7,13,23], and the decrease in the experimental desalination rate was due to the uptake of these organic pollutants.

3.2.2. SEM-EDS analysis

Changes in the morphological features of the film surface were significantly observed in the SEM and AFM images (Fig. 4). It can be clearly seen that the inorganic salt contaminants are unevenly embedded in the organic membrane, and the uneven appearance increases with increasing contamination time, while larger size salt particles are more often deposited on the relatively smooth membrane surface. Moreover, the types and amounts of elements distributed on the membrane surface were analyzed by EDS. The proportions of C, O and Cl all changed to some extent along with the experimental operation. For example, Cl weight increased from 4.06% (original) to 6.05% (Run 1) and 10.68% (Run 2), indicating that contaminants consisted of dichloromethane, dichloroacetaldehyde, chloromethylsulfonyl chloride contributed to the fouling of AFM.

Due to the precipitation or crystallization of contaminants adhering to the membrane surface, the roughness of the contaminated membranes gradually increased, and the peaks became larger, with the value of Rq increasing by more than 3 times (from 6.18 to 20.7 nm). Under the combined effect of staggered flow shear and pressure driving force on the membrane surface, more inorganic salt crystals or precipitates filled in the valleys, while the adsorption of dichloromethane on the valleys and peaks made the membrane surface less smooth [11,13]. At the same time, dichloromethane, dichloroacetaldehyde and chloromethylsulfonyl chloride adsorbed on the surface had a certain hydrophobicity, which can further better illustrate the increase of contact angle.

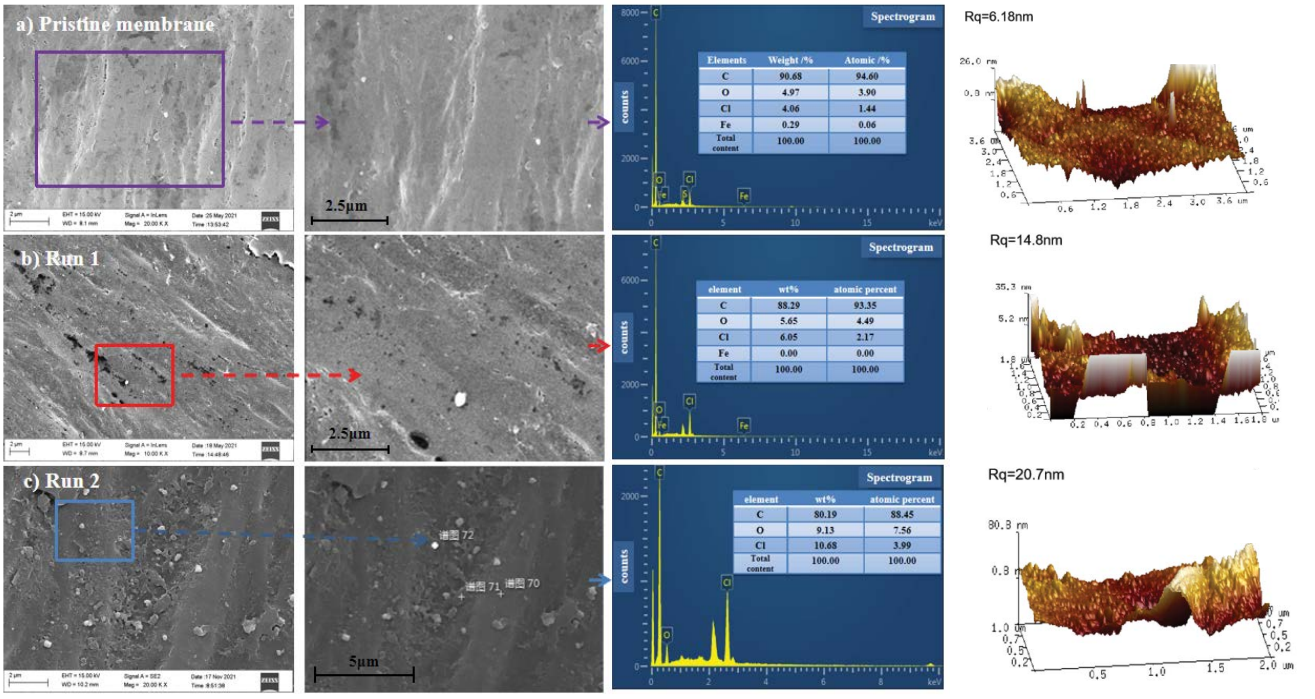

Fig. 4. SEM-EDS and AFM images of (a) original membrane, (b) Run 1 and (c) Run 2.

3.2.3. ATR-FTIR analysis

It can be seen from Fig. 5 that both the original and the foulant membranes showed peaks at 2,871 cm^{-1} (C–H stretching vibration), 2,918 cm^{-1} (CH_2 stretching vibration) and 2,955 cm^{-1} (CH_3 stretching vibration). Compared with the original membrane, the stretching vibration intensity of the three characteristic peaks for Runs 1 and 2 was significantly weaker. The binding energy of carbon–hydrogen bonds was smaller and unstable than that of carbon–chlorine bonds, which was easily to be replaced by the latter [17,18]. The peak of 1,725 cm^{-1} was the characteristic peak of C=O. The reduction of its stretching vibration intensity was caused by the rupture of the carbon–oxygen double bond. Peaks at 1,460 and 1,375 cm^{-1} represented the C=C stretching vibration, and its vibration intensity decreased, while the peak at 1,160 cm^{-1} increased (C–C stretching vibration). According to the reports [8,12,20], the energy contained in C=C is much higher than that of C–C, and substances with lower energy were always more stable than those with higher energy. As the contamination time increased, the vibration intensity of each peak intensified, indicating that more contaminants were adsorbed to the membrane. Overall, the changes in the areas of these three characteristic peaks were consistent with previous reports [5,14].

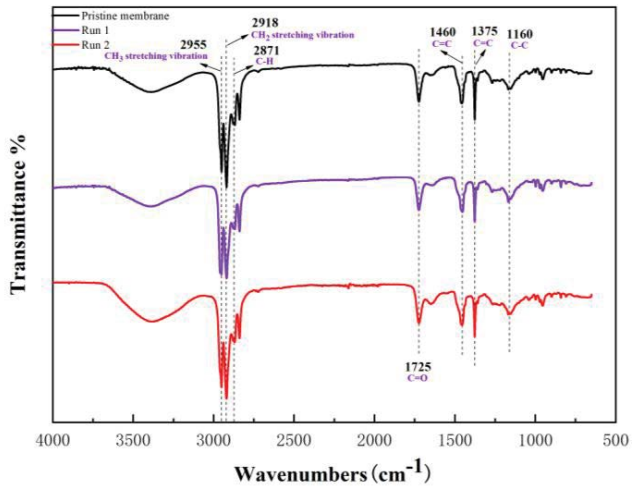

Fig. 5. ATR-FTIR spectrum.

3.2.4. XPS analysis

The XPS spectroscopy was used to further analyze the element content and bonding information. The C1s spectrum was deconvoluted into three peaks at 284.8, 285.7 and 289 eV (Fig. 6), which were attributed to the C–C, C=C and C=O species, respectively. The changes in the areas of these three characteristic peaks were consistent with the results from FTIR. Furthermore, the Cl2p spectrum was deconvoluted into three peaks, all of which were attributed to the organic Cl species. However, the Cl2p spectrum was deconvoluted into four peaks, which were attributed to organic Cl species and metal chloride, respectively. Attributing to the reaction of Cl^- with certain substances, such as Fe^{2+}, the covered areas of organic Cl decreased for Runs 1 and 2.

3.3. Mechanism of membrane fouling and regeneration strategy

The surface of the original membrane was smooth, and mainly composed of polytetrafluoroethylene, styrene and

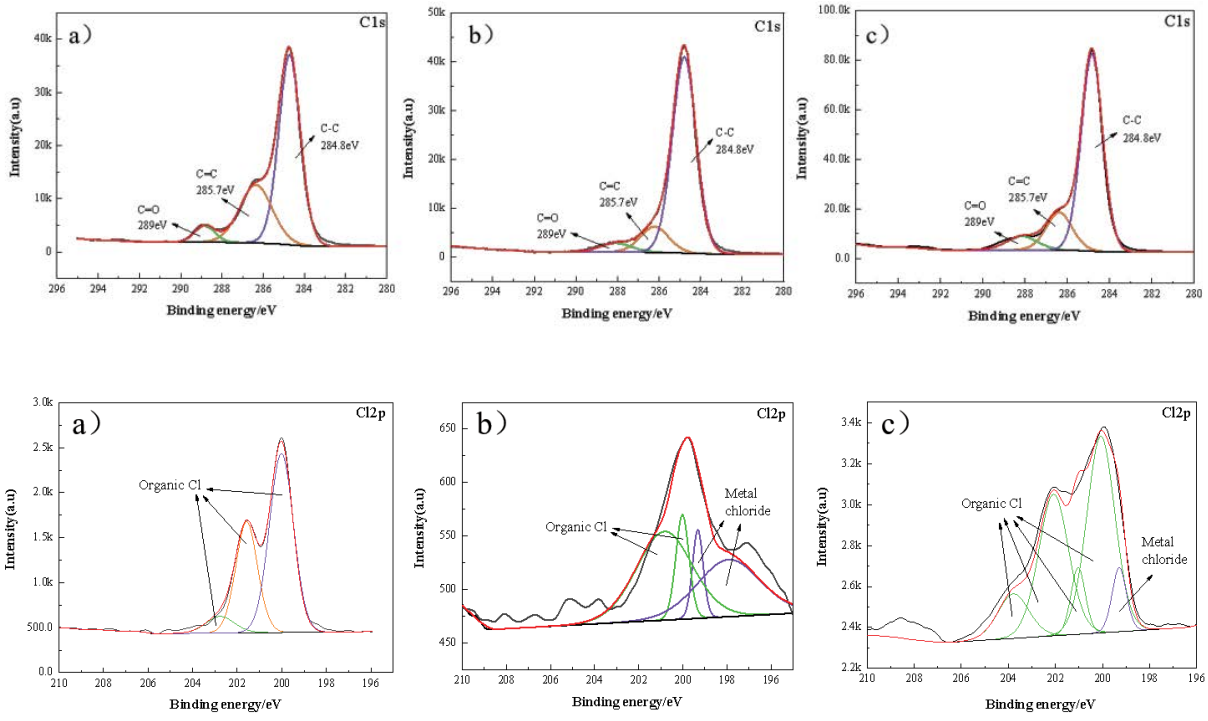

Fig. 6. XPS spectrum of C1s and Cl2p: (a) original membrane, (b) Run 1 and (c) Run 2.

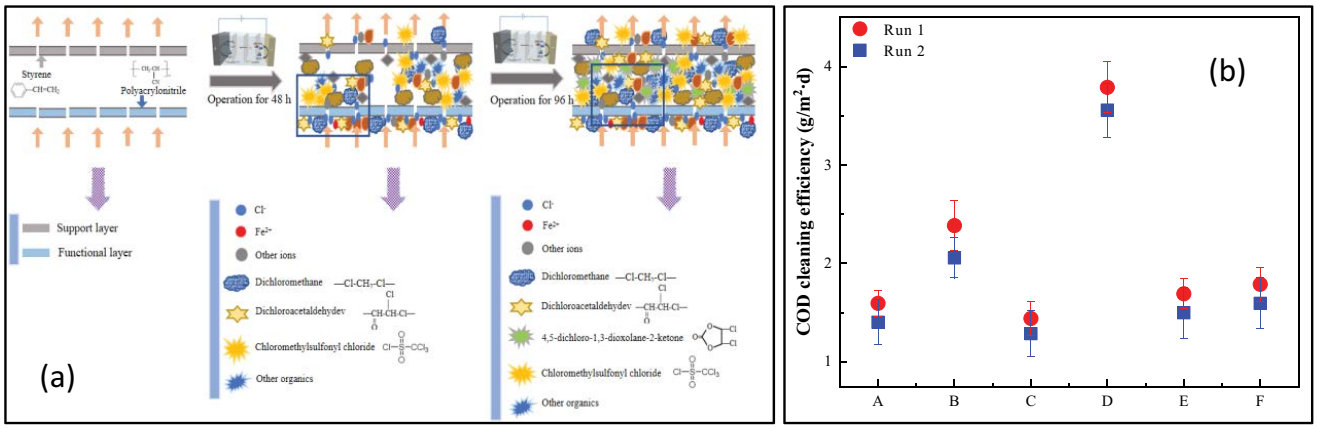

Fig. 7. (a) Mechanism of membrane fouling and (b) foulants removal efficiency.

polyacrylonitrile (Fig. 7a). When the fouling experiment extended to 48 h, its morphology and composition changed significantly. Some pollutants adsorbed on the surface or inside of the ion membrane mainly includes: dichloromethane, dichloroacetaldehyde, chloromethylsulfonyl chloride and other contaminants. Theoretically, cations will not pass through the anion exchange membrane, so Fe^{2+} attached to the membrane surface will not be adsorbed into the inner membrane. The attachment of some hydrophobic organic species resulted in a significant increase in the contact angle. When the continuous operation lasted for 96 h, more inorganic and organic pollutants were found on the surface and inside of the anion exchange membrane, and the number of internal pollutants increased significantly, indicating the deposition of inorganic salts and the adsorption of organic pollutants were the key factors in the long-term operation.

As seen from Fig. 7b, after 96 h of continuous membrane fouling experiments, DI water cleaning only removed 1.59 ± 0.08 g·COD/m²·d, indicating that after a period of fouling, the interaction established between the substance and the membrane was stronger than the physical washing power [21]. Among all the configurations, method D (0.1% NaOH followed by 0.025% Na-SDS) was most efficient in removing the organic pollutant (4.06 ± 0.26 g·COD/m²·d for Run 1 and 3.78 ± 0.22 g·COD/m²·d for Run 2), which was ~3.1 times of method A. According to the COD cleaning efficiency, it was reasonable to conclude that the combination of 0.1% NaOH and 0.025% Na-SDS was efficient in removing the hydrophobic compounds, indicating that a high proportion of hydrophobic substances existed in foulants, which further explained the change of contact angle summary in 3.2.1.

4. Conclusions

Evolution of AEM fouling and regeneration strategy in cold-rolling wastewater treatment by ED were explored in this study. The main findings are as follows: contact angles increased from 90.8° (0 h) to 105° (48 h) and 109° (96 h). The results of SEM-EDS, AFM, ATR-FTIR and XPS explained in detail how the elements and functional groups of the ion membrane changed. Further, the changes in electrical resistance and Cl^- recovery rate were measured and confirmed that the AEM was gradually polluted within 96 h. After 96 h operation, the resistance of desalination compartment increased by 10.42%, while Cl^- recovery rate decreased by 14.01%. Based on the pollution mechanism and data of COD removal, the combination of 0.1% NaOH and 0.025% Na-SDS was suggested, which could remove the hydrophobic compounds and restore the membrane filtration capacity efficiently. Under the optimal conditions, 4.06 ± 0.26 g·COD/m²·d was removed.

Acknowledgement

This work was supported by the China National Key R&D Program [Grant Number 2019YFC1803802].

References

[1] G.Y. Jiang, H.D. Li, M. Xu, H.M. Ruan, Sustainable reverse osmosis, electrodialysis and bipolar membrane electrodialysis application for cold-rolling wastewater treatment in the steel industry, J. Water Process Eng., 40 (2021) 101968, doi: 10.1016/j.jwpe.2021.101968.

[2] A. Campione, L. Gurreri, M. Ciofalo, A. Tamburini, A. Cipollina, Electrodialysis for water desalination: a critical assessment of recent developments on process fundamentals, models and applications, Desalination, 434 (2018) 121–160.

[3] Y. Muhammad, W. Lee, Zero-liquid discharge (ZLD) technology for resource recovery from wastewater: a review, Sci. Total Environ., 681 (2019) 551–563.

[4] H.X. Lu, L. Wang, R. Wycisk, P.N. Pintauro, S.H. Lin, Quantifying the kinetics energetics performance tradeoff in bipolar membrane electrodialysis, J. Membr. Sci., 612 (2020) 118279, doi: 10.1016/j.memsci.2020.118279.

[5] A. Hassanvand, K.J. Wei, S. Talebi, G.Q. Chen, S.E. Kentish, The role of ion exchange membranes in membrane capacitive deionisation, Membranes, 7 (2017) 54–64.

[6] A.A. Uliana, N.T. Bui, J. Kamcev, M.K. Taylor, J.J. Urban, J.R. Long, Ion-capture electrodialysis using multifunctional adsorptive membranes, Science, 372 (2021) 296–299.

[7] P. Malek, J.M. Ortiz, H.M.A. Schulte-Herbrüggen, Decentralized desalination of brackish water using an electrodialysis system directly powered by wind energy, Desalination, 377(2016) 54–64.

[8] K.J. Min, J.H. Kim, K.Y. Park, Characteristics of heavy metal separation and determination of limiting current density in a pilot-scale electrodialysis process for plating wastewater

treatment, Sci. Total Environ., 757 (2021) 143762, doi: 10.1016/j.scitotenv.2020.143762.
[9] X. Xu, Q. He, G. Ma, H. Wang, N. Nirmalakhandan, P. Xu, Selective separation of mono-and di-valent cations in electrodialysis during brackish water desalination: bench and pilot-scale studies, Desalination, 428(2018) 146–160.
[10] H. Yan, Y. Wang, L. Wu, M.A. Shehzad, C. Jiang, R. Fu, Z. Liu, T. Xu, Multistage-batch electrodialysis to concentrate high-salinity solutions: process optimization, water transport, and energy consumption, J. Membr. Sci., 570 (2019) 245–257.
[11] P. Nazila, M. Ahmad, M-Z. Arjomand, M. Mohammad Ali, Recovery of lithium ions from sodium-contaminated lithium bromide solution by using electrodialysis process, Chem. Eng. Res. Des., 98 (2015) 81–88.
[12] E. Mahendiravarman, D. Sangeetha, Anti-biofouling anion exchange membrane using surface modified quaternized poly(ether imide) for microbial fuel cells, J. Appl. Polym. Sci., 134 (2017) 44432, doi: 10.1002/app.44432.
[13] W.C. Lin, M.C. Li, Y.H. Wang, X.M. Wang, K. Xue, K. Xiao, X. Huang, Quantifying the dynamic evolution of organic, inorganic and biological synergistic fouling during nanofiltration using statistical approaches, Environ. Int., 133 (2019) 105201, doi: 10.1016/j.envint.2019.105201.
[14] D. Golubenko, A. Yaroslavtsev, Development of surface-sulfonated graft anion-exchange membranes with monovalent ion selectivity and antifouling properties for electromembrane processes, J. Membr. Sci., 612 (2020) 118408, doi: 10.1016/j.memsci.2020.118408.
[15] F. Tang, H.Y. Hu, L.J. Sun, Y.X. Sun, J.C. Crittenden, Fouling characteristics of reverse osmosis membranes at different positions of a full-scale plant for municipal wastewater reclamation, Water Res., 90 (2016) 329–336.
[16] W.Y. Wang, R.Q. Fu, Z.M. Liu, H.Z. Wang, Low-resistance anti-fouling ion exchange membranes fouled by organic foulants in electrodialysis, Desalination, 417 (2017) 1–8.
[17] Z.J. Zhao, S.Y. Shi, H.B. Cao, Y.J. Bart, V.D. Bruggen, Comparative studies on fouling of homogeneous anion exchange membranes by different structured organics in electrodialysis, J. Environ. Sci., 77 (2019) 218–228.
[18] L. Yao, L. Zhang, R. Wang, S. Chou, Z. Dong, A new integrated approach for dye removal from wastewater by polyoxo-metalates functionalized membranes, J. Hazard. Mater., 301 (2016) 462–470.
[19] C. Zhao, T. Song, Y. Yu, L. Qu, J. Cheng, W. Zhu, Q. Wang, P. Li, W. Tang, Insight into the influence of humic acid and sodium alginate fractions on membrane fouling in coagulation-ultrafiltration combined system, Environ. Res., 191 (2020) 110228, doi: 10.1016/j.envres.2020.110228.
[20] Z. Zhao, S. Shi, H. Cao, B. Shan, Y. Sheng, Property characterization and mechanism analysis on organic fouling of structurally different anion exchange membranes in electrodialysis, Desalination, 428 (2018) 199–206.
[21] M.N. Fini, J. Zhu, B.V.D. Bruggen, H.T. Madsen, J. Muff, Preparation, characterization and scaling propensity study of a dopamine incorporated RO/FO TFC membrane for pesticide removal, J. Membr. Sci., 612 (2020) 118458, doi: 10.1016/j.memsci.2020.118458.
[22] K. Khoiruddin, D. Ariono, S. Subagjo, I.G. Wenten, Improved anti-organic fouling of polyvinyl chloride-based heterogeneous anion-exchange membrane modified by hydrophilic additives, J. Membr. Sci., 41 (2021) 102007, doi: 10.1016/j.jwpe.2021.102007.
[23] X.M. Zhang, C.L. Zhang, F.N. Meng, C.H. Wang, P.F. Ren, Q. Zou, J.Y. Luan, Near-zero liquid discharge of desulfurization wastewater by electrodialysis-reverse osmosis hybrid system, J. Water Process Eng., 40 (2021) 101962, doi: 10.1016/j.jwpe.2021.101962.